Jurnal Teknologi

Full Paper

NUMERICAL ANALYSIS OF SWIRL INTENSITY IN TURBULENT SWIRLING PIPE FLOWS

Khairul Fikri Tamrin[a], Nadeem Ahmed Sheikh[b], Bahbibi Rahmatullah[a*]

[a]Computing Department, Universiti Pendidikan Sultan Idris, 35900 Tanjung Malim, Perak, Malaysia
[b]Department of Mechanical Engineering, Muhammad Ali Jinnah University, Islamabad, Pakistan

Article history
Received
1 February 2015
Received in revised form
24 March 2015
Accepted
1 August 2015

*Corresponding author
bahbibi@fskik.upsi.edu.my

Graphical abstract

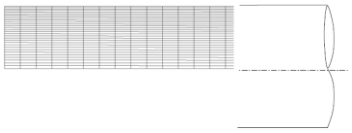

Abstract

Swirling flows are often observed in nature such as weather systems, cyclones and tornados. A number of applications use swirling nature of flow for enhanced mixing, heat transport and other transport phenomena. Naturally occurring swirls as well as induced swirls are often usually turbulent in nature. Understanding the flow physics of turbulent swirling flow is important for better understanding and control of processes involving swirling flows. With the increase of computational resources and advancements in turbulent flow modelling, it is now possible to simulate highly complex flow structures. Here turbulent swirling flow induced by guide vanes is studied using Computational Fluid Dynamics (CFD) simulations in a two-dimensional axisymmetric channel. The results for the variation of velocity components are compared with the work of an earlier research. The results are initially compared for the evaluation of best discretisation scheme. It was observed that the second-order and third-order schemes produced similar results. To simulate the turbulent flow two equations (*k-ε)* model and the five equations Reynolds Stress Model (RSM) are used. The comparison of both models with higher order discretisation schemes shows that the standard k-ε model is incapable of predicting the main features of the flow whilst RSM yields result close to the experimental data.

Keywords: Swirling flow, numerical simulation, turbulence model, standard *k-ε* model, RSM model

Abstrak

Aliran berpusar sering diperhatikan dalam alam semula jadi seperti dalam sistem cuaca, siklon dan puting beliung . Beberapa aplikasi menggunakan aliran berpusar telah digunakan untuk meningkatkan hasil percampuran, pengangkutan haba dan fenomena pengangkutan yang lain. Aliran berpusar juga sering terjadi dalam alam semula jadi. Memahami fizik aliran aliran berpusar adalah penting untuk memahami dan mengawal proses yang melibatkan aliran berpusar. Dengan peningkatan sumber pengiraan dan kemajuan dalam model aliran bergelora, ia kini mungkin untuk meniru struktur aliran yang sangat kompleks. Aliran berpusar yang dihasilkan oleh bilah pandu dikaji menggunakan Dinamik Bendalir Komputeran (CFD) simulasi dalam saluran simetri sepaksi dua dimensi. Keputusan bagi mengubah komponen halaju dibandingkan dengan kerja sebelum ini. Keputusan pada mulanya dibuat perbandingan untuk menilai skim pendiskretan terbaik. Diperhatikan bahawa skim tertib kedua dan ketiga menghasilkan keputusan yang sama. Untuk mensimulasikan aliran berpusar dua persamaan (k-ε) model dan lima persamaan Reynolds Tekanan Model (RSM) digunakan. Perbandingan kedua-dua model dengan skim pendiskretan yang lebih tinggi menunjukkan bahawa model k-ε standard tidak mampu meramalkan ciri-ciri utama aliran manakala keputusan RSM lebih dekat dengan data eksperimen.

Kata kunci: Aliran berpusar, simulasi numerical, model turbulen, model asas *k-ε*, model RSM

1.0 INTRODUCTION

Flow with swirl has been widely utilized in numerous engineering applications especially to enhance heat transfer, species transport and mixing. It has been the subject of an ongoing study either through experimental [1-3] and/or numerical [1, 4-8] means. In general swirl in a flowing medium is generated by imparting an additional component to the flow in the tangential direction. The mechanism of swirling is profound involving highly turbulent flow and has been used to good effect. Many studies on various methods of inducing swirling flows have been reported in the literature. Several techniques include (i) the introduction of the fluid stream by means of one or several tangential inlets into a cylindrical duct [9] (ii) the rotation imparting device resulting in a swirling motion to the fluid as it passes through [10] and (iii) the flow through vanes guiding the flow in an axial tube [11, 12].

One of the most fundamental work on the swirling flows was carried out by Chang *et al.* [13] using multiple tangential injections of fluid at the tube inlet to produce swirling air flow. Chang and Dhir reported two sets of experiments using four and six tangential injectors for the induction of swirl. In comparison to the axial velocity profile, the results indicated that the flow reversal occurs in the central region of tube. In such a case the magnitude of axial velocity was observed to increase near the wall. In relation to tangential velocity, a shifting trend was produced; location of its peak moves radially inwards with increase of distance. Work of Chang and Dhir has been used by a number of researchers to compare results using computational fluid dynamics and explain the fundamental principles behind swirling flows. For instance, using numerical simulations Jiajun *et al.* [14] modelled the flows in a three-dimensional cylindrical pipe induced by several tangential inlets with different initial swirl intensities. The numerical results to extent matched the experimental results presented by Chang *et al.* [13].

In another study, Kitoh [11] experimentally investigated confined swirling flow which was generated using variable guide vanes. It was observed that the swirling component was exponentially decaying downstream due to wall friction and the decay coefficient was seen dependent on swirl intensity. The result of axial velocity showed a flow reversal in the core region. Meanwhile, the tangential component of the velocity shows three categories (i) core region, (ii) annular region, and (iii) near wall regions. Since the first region was dominated by a forced vortex motion, the radial velocity component seems to be negligible in comparison to other components.

Modelling the nature of swirling flow is quite challenging due to varying turbulent intensity and length scales. Several researchers have computed the properties of swirling flow in simple geometries such as pipes and ducts by employing various turbulence models. It was reported that swirling motion of fluid may results in increased anisotropy of stress and dissipation tensors [11]. The higher dissipation is likely to cause anisotropic eddy viscosity [15]. For these reasons, k-ε model is unlikely to perform well in such flow conditions.

A comprehensive review on modelling swirling flows is carried out by Sloan *et al.* [16]. Sloan concluded that the performance of two equation turbulence model in the vicinity of recirculation zones was poor primarily due to swirling flows exhibiting highly three-dimensional structures. The inherent weaknesses associated with the standard k-ε model in predicting behaviour of turbulence in these conditions have led researchers to employ other turbulence models with different closures. Several researchers who have utilised RSM reported considerable degree of success in predicting swirling flows.

Early numerical work of a swirling jet using five equations was conducted by Gibson *et al.* [17] but the result obtained was insufficient to evaluate the capability of RSM's prediction since the effect of wall was excluded. On the other hand, Weber *et al.* [18] simulated confined swirling flows using three turbulence models; k-ε, RSM and ASM. However, k-ε model was incapable to correctly estimate turbulence production and the pattern of tangential momentum [19]. The other two models produced reasonable conformity with the experimental data but not for the case of predicting reversal flows.

The generation of reversed flow strongly depends on the swirl strength. Swirl number, *S*, is usually used to account for the strength of the swirl. It is defined as [20],

$$S = \frac{G_\phi}{G_x R_o} = \frac{\int_0^R U W r^2 dr}{R \int_0^R U^2 r\, dr} \quad (1)$$

where G_ϕ is the swirl momentum, G_x is the axial flux linear momentum and R_o is the characteristic length, usually the radius of pipe.

$$G_\phi = \int_0^R (W r) \rho U 2\pi r\, dr = \text{constant} \quad (2)$$

$$G_x = \int_0^{r_o} U \rho U 2\pi r\, dr + \int_0^{r_o} p\, 2\pi r\, dr = \text{constant} \quad (3)$$

Alternatively, Kitoh [11] has defined the swirl number as

$$S = 2\pi\rho\int_0^{r_o} U W r^2 dr / \rho\pi R_o^3 U_m^2 \quad (4)$$

where U_m is the bulk axial velocity and the flow Reynolds number Re = $U_m D/\nu$ using kinematic viscosity, ν of fluid.

Swirl plays an important role to increase the entrainment rate and velocity decay rate [20]. In general, the strength of swirl can be categorized as either weak swirl (S < 0.6) or strong swirl (S > 0.6). Poor internal circulation is noted in weak swirling system due to low axial pressure gradients. While strong swirl has adverse pressure gradient along the flow axis leading to the formation of recirculation zone in the central region of the form of toroidal vortex [20]. The recirculation zone however varies in width and length depending on the swirl strength.

In light of the above discussion, it can be safely concluded that simulating the highly turbulent swirling flow is quite difficult. In past few decades a number of efforts have been made to predict the exact nature of flow. However mostly these efforts have been hindered by the inability of turbulent models and or computational resources. With the recent advancements in computational fluid dynamics and turbulence modeling, modeling such flows is deemed possible. This work also uses the latest turbulent models to capture the flow physics in a simple geometry. Results for the velocity distributions along the pipe are compared with the experimental data.

2.0 METHODOLOGY

2.1 Governing Equations

The swirling flow in this study is considered to be axisymmetric two-dimensional, steady and incompressible. The swirl induced by guide vanes is based on the conservation of mass and momentums. There are two conservation principles which govern the flow being studied: (a) conservation of mass: and (b) conservation of momentum described using Navier-Stokes equations. Nonetheless, the conservation of energy is neglected since the flow is assumed to be independent of heat transfer and temperature.

2.2 Numerical Models

In swirling flows, Turbulence is formed due to random flow fluctuation of fluid velocity in addition to rotating eddies interfere with steady mean flow. These random fluctuations occur over very small distances in space and time compared to overall domain. Computational grid domain and refinement must be smaller than the smallest element of eddy but should cover the entire control volume so that eddy can be modelled accurately.

In present simulation, steady mean flow is analyzed by averaging velocity and pressure over a time scale. The equations describing the flow are in terms of the mean velocity and pressure. However, these equations contain unknown quantities representing the Reynolds stress and transport of mean momentum which require additional equations to solve for all parameters. Therefore, turbulence modelling comes into context tries to solve the Navier-Stokes equations, the continuity equation and few additional differential equations. Two turbulence models were employed for these simulation; standard two equations k-ε and five equations RSM models.

2.2.1 k-ε Model

The standard two equations k-ε model offers economical computational time and cost, robustness and provides rational comparisons for a wide range of turbulent flows. It is also a semi-empirical model and many studies have been conducted to make some improvements in its performance. In contrast to laminar flow, turbulent flow calculations are governed by two additional parameters which are turbulent kinetic energy, k and dissipation rate ε.

2.2.2 RSM Model

Based on the suggestion given by Kitoh [11], RSM was employed for modelling swirling flows. RSM eliminates the isotropic eddy-viscosity hypothesis and solves for individual Reynolds stresses in addition to the dissipation term ε [21]. In brief, RSM employs adequate number of transport equations for the Reynolds stresses in two-dimensional together with additional equation for the rate of dissipation. In terms of computational cost, RSM is relatively expensive to run.

3.0 EXPERIMENTAL BACKGROUND

For the purpose of comparison, experimental results of Kitoh [11] are used. The experimental setup consisted of a hydraulically smooth internal pipe surface with 150 mm internal diameter and 7000mm length. A hot-wire anemometer was used to measure the instantaneous flow velocities and respective distributions of Reynolds stresses along the pipe. Air was used as a working fluid and a swirl generator was installed at the upstream end of the pipe along with a settling chamber. The 24 vanes generator imparts swirling component to the flow as it passes radially inward. Swirl intensities of various magnitudes can be achieved by changing the vane angles with respect to the radial direction. A variable-speed motor was used to adjust the flow rate which was measured

using a venturi meter. The experimental Reynolds number was kept at 50,000. A number of test sections (TS) were made along the pipe to probe flow mean velocities and angles using hot-wire probes. Table 1 summarizes the data obtained using the setup.

Table 1 Test sections and the corresponding swirl intensities. The numbers indicate swirl number, *S*. The experimental swirl number and velocity results located at x/D = 5.7 was chosen as the inlet boundary conditions for the current simulation. Re stands for Reynolds number.

	TS x/d Re	1 5.7	2 7.7	3 12.3	4 14.3	5 19.0	6 21.0	7 25.7	8 28.0	9 32.4	10 39.0	11 43.3
1	6 x 10^4	-	1.42	-	1.18	-	0.89	-	0.38	0.64	0.57	-
2	6 x 10^4	-	0.71	-	0.58	-	0.53	-	-	0.35	0.36	0.30
3	6 x 10^4	-	0.28	-	0.24	-	0.21	-	-	0.12	0.15	0.14
4	6 x 10^4	-	-	-	-	-	-	-	-	-	-	0.11
5	6 x 10^4	-	-	-	-	-	-	-	-	-	-	0.07
6	8 x 10^4	-	-	-	-	-	-	-	-	-	-	-
7	5 x 10^4	-	-	-	-	-	-	-	-	-	-	-
8	5 x 10^4	0.97	-	0.83	-	0.67	-	0.60	-	0.47	0.42	-
9	5 x 10^4	-	-	0.59	-	-	-	0.43	-	-	0.36	-
10	5 x 10^4	-	-	0.24	-	-	-	0.18	-	-	0.12	-

4.0 BOUNDARY CONDITIONS

Description of inlet velocity profile is important for the determination of flow field in the domain. However exact details for the inlet flow boundary conditions are not found. However, Kitoh [11] has provided the velocity distributions at upstream locations from the experimental inlet for various TS as shown in Table 1. The first test section of Run 8 is chosen as the test conditions for the simulations.

In order to accommodate the exact velocity distributions, the inlet position has been moved upstream towards the test section defined at x/d=5.7 i.e. 855 mm from the inlet (see Figure 1). Velocity profiles for all three components U (axial), V (radial) and W (tangential) were adopted as the boundary conditions profile as provided by Kitoh [11]. Figure 2 shows the velocity profiles for U, V and W components of the velocity. By moving the inlet location upstream with 855 mm offset, the length of simulation domain was reduced to 6145 mm.

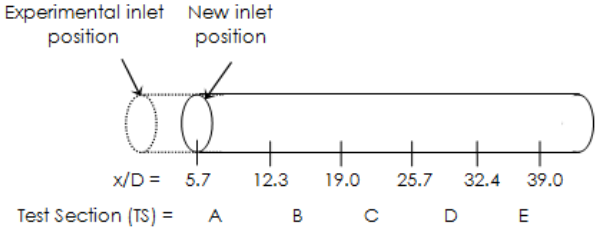

Figure 1 Diagram shows the position of new inlet A and the positions where the velocity from computations will be referring to (B, C, D, E and F).

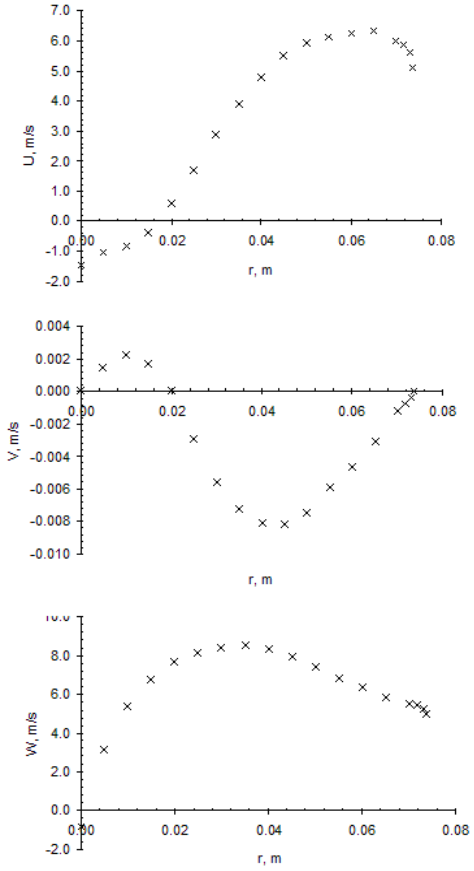

Figure 2 Axial (U), radial (V) and tangential (W) velocity distributions at new inlet position A which are similar with the experimental result obtained at location x/D= 5.7

The experimental data provides no description of turbulence intensities and dissipation. An estimate for the turbulence intensity, *I* and length scale, γ was calculated using an empirical relationship of fully-developed pipe flow, $I = 0.16\ Re^{-1/8}$ [21]. While the length scale was approximated using γ =0.07D [21]. The values for *I* and γ used for the simulation are reported in Table 2.

The normal gradients for all flow variables were assumed zero for the outflow condition. In addition, for the wall conditions, the simulation uses standard wall functions as proposed by Launder *et al.* [22].

Table 2 Initial turbulence quantities

Parameter		Value
Turbulence intensity, *I*	4.14%	for Re = 50,000
Turbulence length scale, γ	0.0105	for D = 0.150m

5.0 SIMULATION GEOMETRY

A two-dimensional axisymmetric domain was used for all simulations. The grid was constructed uniformly in the axial direction but progressively refined in the radial direction with aspect ratio of 0.975 where mesh is created denser near the wall (see Figure 3). In order to obtain grid independence, subsequent refinements were performed by doubling the grid points in each x- and y-direction. Four different grid sizes were employed to conduct grid sensitivity analysis for k-ε turbulence model. Variations of axial, radial and tangential velocity components of swirling pipe flow located at x/D = 25.7 are displayed to determine grid independence (see Figure 4). Detail of grid sizes is presented in Table 3.

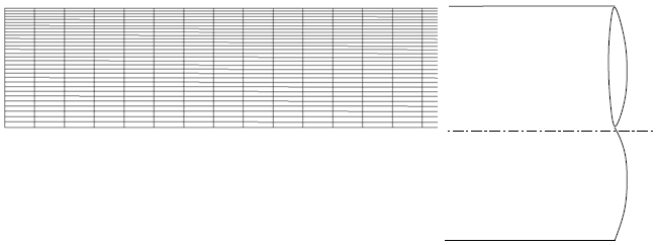

Figure 3 Two-dimensional axisymmetric grid for turbulent swirling flow pipe

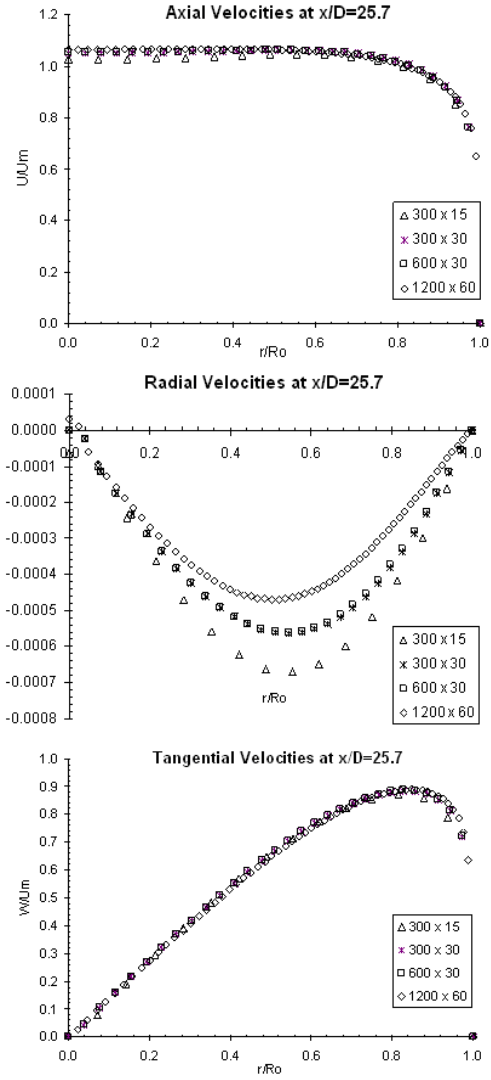

Figure 4 Comparison of axial, radial and tangential velocity components for different grid configurations

Table 3 Successive grid refinement in the x- and y-direction respectively

Grid Refinement	Mesh	Aspect Ratio
Level 1	300 by 15	0.975
Level 2	300 by 30	0.975
Level 3	600 by 30	0.975
Level 4	1200 by 60	0.975

Axial and tangential velocity distributions show some degree of agreement Variations of radial velocity component is used to determine the grid independence. It was observed that grid size of 300x30 and 600x30 show grid independent. Therefore grid size of 300x30 is chosen for further computation with half the computational time of 600x30 grid size.

6.0 VALIDATION SIMULATIONS AND TURBULENCE MODELS

6.1 Discretisation Schemes

The results for the simulation are compared using five different discretisation schemes: (a) first-order upwind, (b) second-order upwind, (c)Power-Law, (d) QUICK and (e) third-order MUSCL. Detailed descriptions of the schemes can be found in [21].

The computation was conducted by employing each discretisation scheme at a time with the comparison of predicted velocity distributions. It can be noticed in Figure 5 that the first-order upwind scheme represents major differences in comparison to the other schemes, as expected, especially for radial and tangential velocity distributions using standard k-ε model. For radial velocity, an overshoot near the axisymmetric line can also be observed due to the possibility of numerical diffusion. It was concluded that the first-order discretisation scheme is not appropriate for simulating swirling flow problem using k-ε model. In contrary, RSM model does not display any major anomaly for all velocity distributions for the different discretisation schemes (Figure 6). Based on the results of Figure 5 and 6, Second-order upwind was chosen for the simulations.

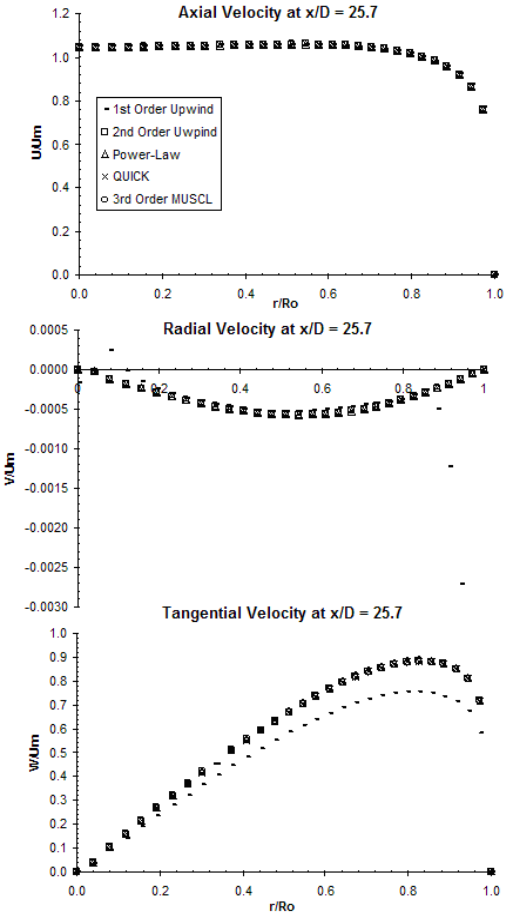

Figure 5 Discretisation schemes with *k-ε* model at x/D=25.7

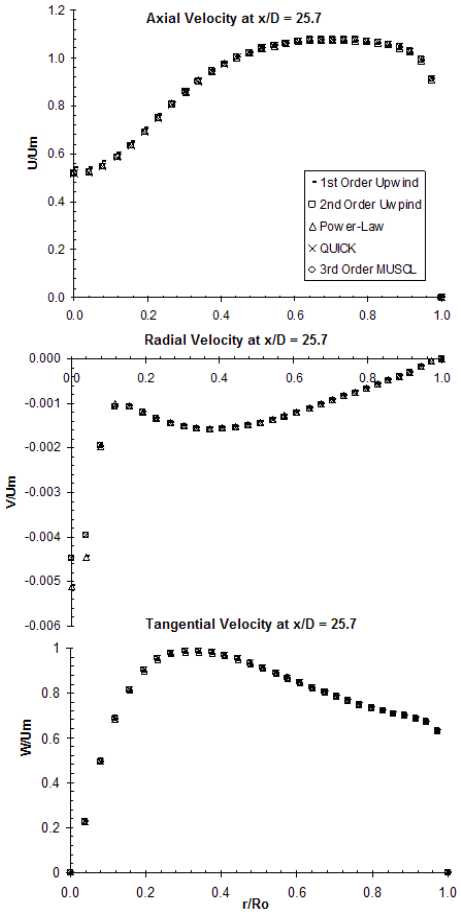

Figure 6 Discretisation schemes with RSM model at x/D=25.7

7.1 RESULTS AND DISCUSSION

In this section, numerical results for the three components of the velocity distributions are presented and compared. The results obtained are based on Reynolds number of 50,000 and initial swirl number 0.97 located at the inlet. Comparison is made using experimental data at axial locations (from B to F).

A quick examination on the computed flow fields near the inlet shows that both turbulence models predict a recirculation zone (see Figure 7 and 8). Figure 7 shows the recirculation zone for *k-ε* model where it predicts at 5.3D upstream relative to the domain inlet. The strength of the swirl is seen higher with *k-ε* model compared to RSM model and show better agreement with experimental data (see Table 4).

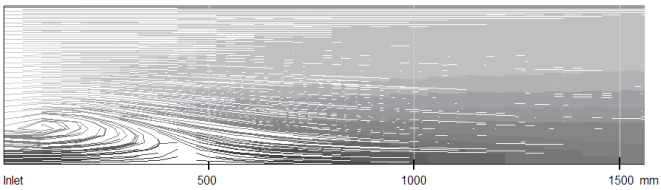

Figure 7 The streamline in the axisymmetric pipe for *k-ε* model

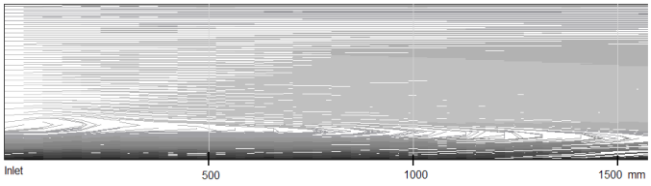

Figure 8 The streamline in the axisymmetric pipe for RSM model

Table 4 Comparison of experimental (Run 8) and computed swirl numbers, *S* at various test sections (TS)

Test section	Experimental	*k-ε*	RSM
B (x/D = 12.3)	0.83	0.81	0.75
C (x/D = 19.0)	0.67	0.64	0.62
D (x/D = 25.7)	0.60	0.52	0.52
E (x/D = 32.4)	0.47	0.43	0.43
F (x/D = 39.0)	0.42	0.35	0.36

7.1 Axial Velocity Distributions

The variations in the axial velocity are shown in Figure 9. The profiles show lower values of velocity in the core region. The surrounding annular region has relatively high velocity. The experimental data reveals a reversal flow in the central region and with the decay of swirl the magnitude of the reverse flow also decreases [11]. However, in the central portion of the pipe flow reversal was not predicted during the computation in both models. In fact, in the central region RSM shows an increase of axial velocity as the swirl decays. That could be the reason RSM was unable to forecast the formation of central recirculation zone.

The standard *k-ε* model predicted flat axial velocity profiles in the entire core and annulus regions. Due to the effect of wall friction, similar velocity patterns are observed duplicating the experimental data. In general, RSM is able to correctly predict the experimental results across the annulus region and to the wall.

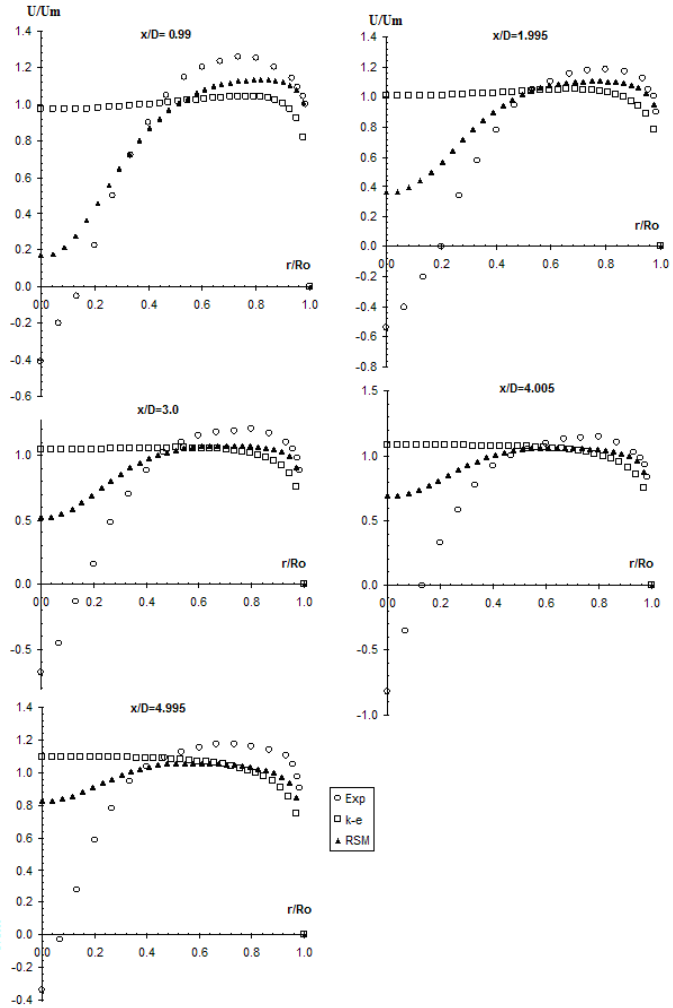

Figure 9 Axial velocity distributions at various axial locations

7.2 Radial Velocity Distributions

In general, radial velocity is seen to be distributed in the range of three orders of magnitude smaller than the reported axial velocity (see Figure 10). It can be understood that radial velocity is insignificant in the swirling flow analysis. This indicates that the mean flow is primarily two-dimensional in the 'x-θ' plane [23]. This further implies that any small error in axial velocity has a large effect on the radial momentum equation due to the preservation of mass continuity [23].

Assessment on turbulence model shows that RSM model failed to predict the main flow physics especially in the centre region of pipe. Theoretical studies and experimental results validate that radial velocity at the pipe centre should be zero since r = 0. Apart from that, there are typical undershoots at r/Ro $\approx$ 0.16 not seen in *k-ε* model and the literature. However, near the region of maximum tangential velocity, RSM predicts a negative local maximum of radial velocity in the annular region. It can also be seen that *k-ε* model closely predict the shape of

radial distribution in the core region and near the wall. The magnitude of maximum radial velocity reported by *k-ε* model is much less than in the literature.

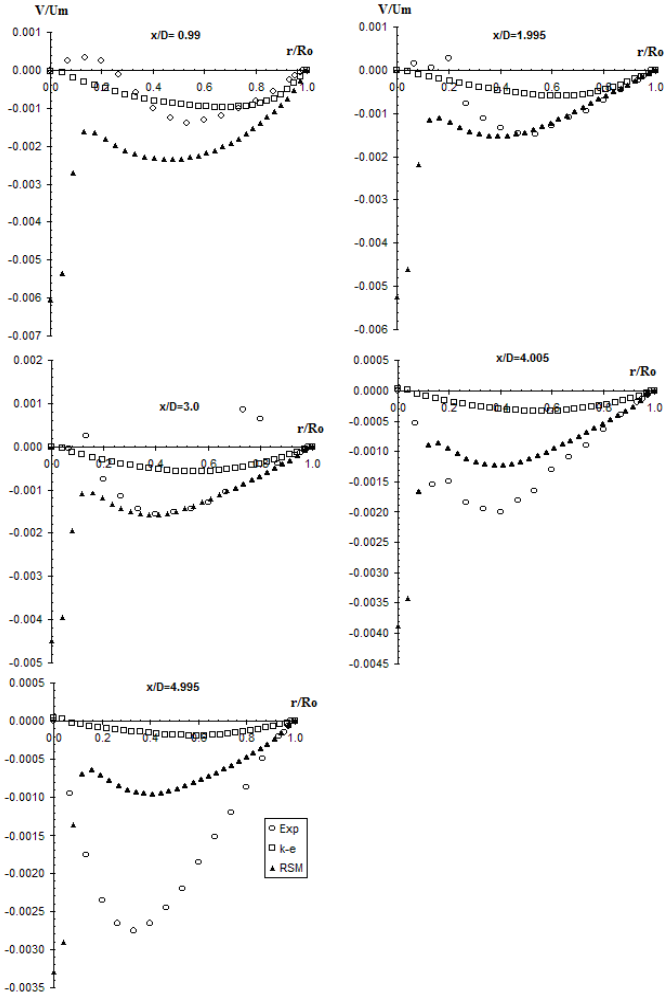

Figure 10 Radial velocity distributions at various axial locations

7.3 Tangential Velocity Distributions

Experiment shows that the tangential velocity decreases with radial variations in the annular region and keep on decreasing as the swirl decays (see Figure 11). Its peak value is reported occurring near the core region and moves towards centreline with decaying swirl further downstream.

Conversely, the RSM reveals that tangential velocity has a local maximum, the magnitude at which decreases gradually with distance far downstream. Comparison of predicted and measured tangential velocity for RSM is in general reasonable. Predictions for the flow physics compares relatively well at location x/D = (0.99, 1.995, 3.0) capturing the sharp changes in the core region and peak values. However, the peak values are largely under predicted for x/D = (4.005, 4.995) where they are located further distance from the core region. In contrast to the experimental data, *k-ε* model radically under predicts the tangential velocity in the annulus and core regions and over predicts the velocity in the region near the wall.

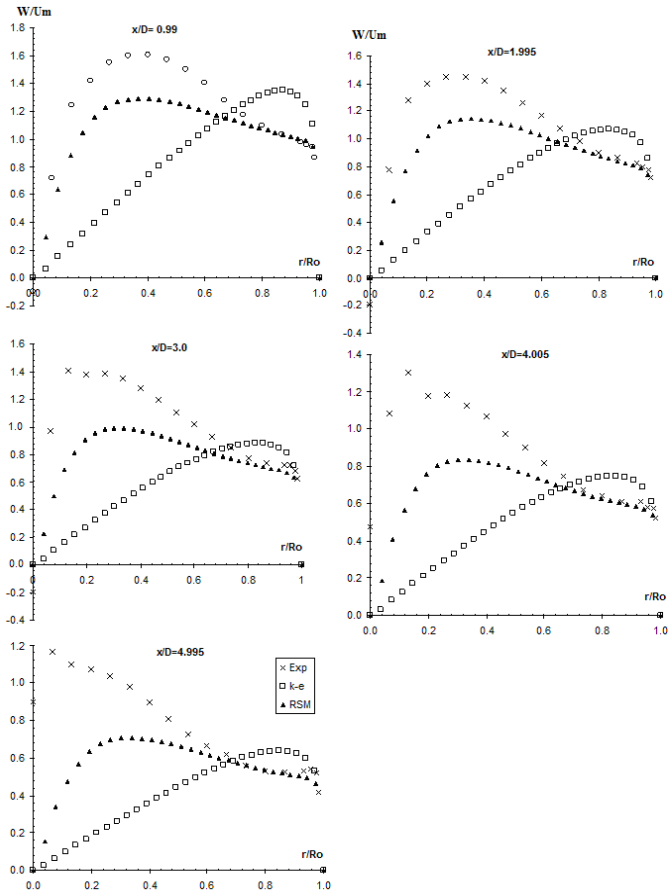

Figure 11 Tangential velocity distributions at various axial locations

8.0 CONCLUSIONS

Modelling turbulent flows is challenging, however due to their vital importance in many natural and industrial processes, understanding their nature is important. Highly turbulent swirling flow presents a significant test for different turbulence models and computational schemes. This work uses different discretisation schemes along with two highly successful turbulence models to simulate highly turbulent swirling pipe flow. It was observed that the higher order discretisation schemes show better results compared to first order schemes. In addition, it was observed that the standard *k-ε* failed to predict main flow features. While RSM model yields better comparison with experimental results by simulating major features of swirling flow. The main distinction between *k-ε* model and RSM is the ability to predict the recirculation zone near the pipe axis. The work shows the ability of capabilities of the latest CFD

techniques and their usefulness in simulating highly turbulent swirling flows.

Acknowledgement

This work was supported by the Ministry of Education Malaysia under grant KPM(B) 840521145857; and Sultan Idris Education University (UPSI) under Research Acculturation Grant Scheme (RAGS) 2013-0161-109-72.

References

[1] Ahmadvand, M., Najafi, A., Shahidinejad, S. 2010. An Experimental Study And CFD Analysis Towards Heat Transfer And Fluid Flow Characteristics Of Decaying Swirl Pipe Flow Generated By Axial Vanes. *Meccanica*. 45(1): 111-129.

[2] Ho, K., Abakr, Y.A., Chan, A. 2011. An Experimental Set-Up For Investigating Swirling Decaying Flow In An Annular Pipe. *International Communications in Heat and Mass Transfer*. 38(9): 1253-1261.

[3] Cazan, R., Aidun, C.K. 2009. Experimental Investigation Of The Swirling Flow And The Helical Vortices Induced By A Twisted Tape Inside A Circular Pipe. *Physics of Fluids*. 21(3): 037102.

[4] Sentyabov, A., Gavrilov, A., Dekterev, A. 2011. Investigation Of Turbulence Models For Computation Of Swirling Flows. *Thermophysics And Aeromechanics*. 18(1): 73-85.

[5] Von Lavante, E., Yao, J. 2012. Numerical Investigation Of Turbulent Swirling Flows In Axisymmetric Internal Flow Configurations. *Flow Measurement and Instrumentation*. 25: 63-68.

[6] Ćoćić, A. S., Lečić, M. R., Čantrak, S. M. 2014. Numerical Analysis Of Axisymmetric Turbulent Swirling Flow In Circular Pipe. *Thermal Science*. 18(2): 493-505.

[7] Hreiz, R., Gentric, C., Midoux, N. 2011. Numerical Investigation Of Swirling Flow In Cylindrical Cyclones. *Chemical Engineering Research And Design*. 89(12): 2521-2539.

[8] Najafi, A., Mousavian, S., Amini, K. 2011. Numerical Investigations On Swirl Intensity Decay Rate For Turbulent Swirling Flow In A Fixed Pipe. *International Journal of Mechanical Sciences*. 53(10): 801-811.

[9] Kumar, R., Conover, T. 1993. Flow Visualization Studies Of A Swirling Flow In A Cylinder. *Experimental Thermal And Fluid Science*. 7(3): 254-262.

[10] Hallett, W., Ding, C.Y. 1995. A Momentum Integral Model For Central Recirculation In Swirling Flow In A Sudden Expansion. *The Canadian Journal Of Chemical Engineering*. 73(3): 284-291.

[11] Kitoh, O. 1991. Experimental Study Of Turbulent Swirling Flow In A Straight Pipe. *Journal Of Fluid Mechanics*. 225: 445-479.

[12] Zaherzadeh, N., Jagadish, B. 1975. Heat Transfer In Decaying Swirl Flows. *International Journal Of Heat And Mass Transfer*. 18(7): 941-944.

[13] Chang, F., Dhir, V. 1994. Turbulent Flow Field In Tangentially Injected Swirl Flows In Tubes. *International Journal Of Heat And Fluid Flow*. 15(5): 346-356.

[14] Jiajun, C., Haynes, B.S., Fletcher, D.F. 1999. A Numerical And Experimental Study Of Tangentially Injected Swirling Pipe Flows. *Second International Conference on CFD in the Minerals and Process Industries*. Melbourne, Australia. 6-8 December 1999.

[15] Yajnik, K., Subbaiah, M. 1973. Experiments On Swirling Turbulent Flows. Part 1. Similarity In Swirling Flows. *Journal of Fluid Mechanics*. 60(04): 665-687.

[16] Sloan, D. G., Smith, P. J., Smoot, L. D. 1986. Modeling of swirl in turbulent flow systems. *Progress in Energy and Combustion Science*. 12(3): 163-250.

[17] Gibson, M., Younis, B. 1981. Calculation of a turbulent wall jet on a curved wall with a Reynolds stress model of turbulence. *Proc. 3rd Turbulent Shear Flows Symposium*. Davis, California. 9-11 September 1981. 4(1): 4.6.

[18] Weber, R., Visser, B., Boysan, F. 1990. Assessment Of Turbulence Modeling For Engineering Prediction Of Swirling Vortices In The Near Burner Zone. *International Journal Of Heat And Fluid Flow*. 11(3): 225-235.

[19] Malalasekera, W., Ranga Dinesh, K., Ibrahim, S., Kirkpatrick, M. 2007. Large Eddy Simulation Of Isothermal Turbulent Swirling Jets. *Combustion Science and Technology*. 179(8): 1481-1525.

[20] Beér, J. M., Chigier, N. A. 1972. *Combustion Aerodynamics*. London: Applied Science Publishers Ltd.

[21] Versteeg, H.K., Malalasekera, W. 2007. *An Introduction To Computational Fluid Dynamics: The Finite Volume Method*. Essex: Prentice Hall.

[22] Launder, B. E., Spalding, D. 1974. The Numerical Computation Of Turbulent Flows. *Computer Methods In Applied Mechanics And Engineering*. 3(2): 269-289.

[23] Carroni, R. 1999. Investigation And Validation Of A Cubic Turbulence Model In Isothermal And Combusting Flows. Ph.D Thesis. Loughborough University.